Available online at www.sciencedirect.com
SCIENCE DIRECT®
Finite Elements in Analysis and Design 40 (2004) 241–262
FINITE ELEMENTS IN ANALYSIS AND DESIGN
www.elsevier.com/locate/finel

Finite element analysis and design of actively controlled piezoelectric smart structures

S.X. Xu[1], T.S. Koko*

Research and Emerging Technologies Department, Martec Limited, Suite 400, 1888 Brunswick Street, Halifax, Canada, NS B3J 3J8

Received 21 January 2002; accepted 25 August 2002

Abstract

A general purpose design scheme of actively controlled smart structures with piezoelectric sensors and actuators is presented in this study. The proposed scheme can make use of any finite element code with piezoelectric elements, and control design is carried out in state space form established on finite element modal analysis. Subsequent details of designing state/output feedback control are addressed. For the purpose of demonstration, a commercial finite element code complemented with output feedback control law is employed to design a set of structure systems for active vibration control. The validity and efficiency of present scheme is confirmed by comparing with available reported results. The present scheme can be adapted to the design of actively controlled smart structures with non-piezoelectric sensors or actuators.

Keywords: Smart structures; Finite element analysis; Piezoelectric; Active vibration control; Design tool

1. Introduction

The concept of smart or intelligent structures started a new structural revolution [1]. A smart structure typically consists of a host structure incorporated with sensors and actuators coordinated by a controller. The integrated structure system is called a smart structure because it has the ability to perform self-diagnosis and adapt to the environment change. The technology of smart materials and structures especially piezoelectric smart structures has become mature over the last decade. One promising application of piezoelectric smart structures is the control and suppression of unwanted structural vibrations [2].

* Corresponding author.
E-mail address: koko@martec.com (T.S. Koko).
[1] Current address: Cornell Fracture Group, 641 Rhodes Hall, Cornell University, Ithaca, NY 14853, USA.

0168-874X/$ - see front matter © 2002 Elsevier B.V. All rights reserved.
doi:10.1016/S0168-874X(02)00225-1

The design methodologies of piezoelectric smart structures are now on the cutting edge as researchers are expanding the advantage of these structures to the real life applications [3]. There are two distinctive features in the design of smart structures. On the one hand, the high degree integration of sensors, actuators and host structures requires techniques of modeling hybrid material systems. The finite element method, a widely accepted and powerful tool for analyzing complex structures, is capable of dealing with the integration of smart components and classic structural parts. Special finite elements have been developed to account for piezoelectric effect [4]. Piezoelectric elements have also become available in commercial finite element codes such as ANSYS and ABAQUS. On the other hand, the design of smart structures is multidisciplinary by nature. Design of a smart structure system requires more than accurate structural modeling. To design piezoelectric smart structures for active vibration control, both structural dynamics and control theory need be considered.

Many researchers have developed specialized finite element inhouse codes to deal with piezoelectric smart structures. Tzou and Tseng [5] developed a finite element code incorporated with feedback control design to study the vibration suppression of a flexible shell structure with piezoelectric sensors and actuators. Ha et al. [6] developed an 8-node three-dimensional finite element code COMPZ for analyzing fiber reinforced laminated composites containing piezoceramic sensors and actuators. Koko et al. [7] and Smith et al. [8] presented a 20-node piezoelectric element code SMARTCOM, capable of designing independent modal-space control and state feedback control. Lim et al. [9] employed the output feedback control law in an inhouse code to study the vibration control of a plate structure. The common feature of above analysis/design tools is that the implementation of a control law is carried out through modifying system matrices while formulating finite element equations. Consequently, the implementation of control design becomes an intrinsic part of the developed finite element code. In view of an abundance of existing finite element codes capable of analyzing piezoelectric structures, it is desirable to develop a general purpose design tool that can utilize any existing code and implement a user-selected control algorithm. In addition, utilization of commercial finite element codes can be advantageous in developing smart structures for real-life industrial applications.

The objective of this study is to develop a general purpose analysis and design scheme of actively controlled piezoelectric smart structures. Instead of making control design an intrinsic part of finite element formulation, the proposed scheme can make use of any finite element code capable of piezoelectric analysis. In what follows, the remaining part of the paper is organized into four sections:

- Section 2 deals with finite element modeling of piezoelectric smart structures. The focus is on smart components (piezoelectric material). The global finite element equations of motion are given along with the equations of modal-space model.
- Section 3 details feedback control design of piezoelectric structure systems. Transforming finite element model to state space model is discussed first. Detailed discussions are then presented on how to design an actively controlled system using state feedback control law or output feedback control law.
- Section 4 presents three case studies to demonstrate the validity and efficiency of proposed design scheme. An experimental beam structure is studied first, and the results of present scheme are compared with available experimental results and results from an inhouse code. Practical design issues such as location of sensors and actuators are illustrated in other case studies.
- Finally, some concluding remarks are drawn in Section 5.

2. Structure modeling

The material behavior of sensors and actuators made of piezoelectric materials can be modeled by the following constitutive equations involving two mechanical variables and two electrical variables [10]:

$$\{\sigma\} = [c]\{\varepsilon\} - [e]^{\mathrm{T}}\{E\}, \tag{1}$$

$$\{D\} = [e]\{\varepsilon\} + [\epsilon]\{E\}, \tag{2}$$

where mechanical variable σ and ε denote the stress and the strain, respectively; electrical variable D and E denote the electric displacement and the electric field, respectively. Note that electric displacement (D) and electric field (E) are fundamental variables in the theory of electrostatics [11]. Matrices $[c]$, $[e]$ and $[\epsilon]$ represent material properties: $[c]$ is the elasticity matrix, $[e]$ is the piezoelectric matrix, $[\epsilon]$ is the dielectric matrix.

Note that piezoelectric matrix $[e]$ accounts for the piezoelectric effect, i.e. the intrinsic coupling between mechanical and electric fields. Eq. (1) characterizes the converse piezoelectric effect that enables piezoelectric materials to function as actuators, while Eq. (2) characterizes the direct piezoelectric effect that enables piezoelectric materials to function as sensors.

The material behavior of host structures made of conventional materials can be well modeled by classical constitutive equations. By vanishing the piezoelectric matrix $[e]$, Eqs. (1) and (2) represent classical constitutive equations for structural and electrical fields, respectively.

Variational principles can be used to establish the finite element equations for piezoelectric structures. The global equation of motion governing a structure system with n degrees of freedom can be written as [5]

$$\begin{bmatrix} M_{uu} & 0 \\ 0 & 0 \end{bmatrix} \begin{pmatrix} \ddot{u} \\ \ddot{\phi} \end{pmatrix} + \begin{bmatrix} C_{uu} & 0 \\ 0 & 0 \end{bmatrix} \begin{pmatrix} \dot{u} \\ \dot{\phi} \end{pmatrix} + \begin{bmatrix} K_{uu} & K_{u\phi} \\ K_{u\phi}^{\mathrm{T}} & K_{\phi\phi} \end{bmatrix} \begin{pmatrix} u \\ \phi \end{pmatrix} = \begin{pmatrix} F_u \\ F_\phi \end{pmatrix}, \tag{3}$$

where u denotes structural displacement, ϕ denotes electric potential, and a dot above a variable denotes a time derivative; M_{uu} is the structural mass matrix, C_{uu} is the structural damping matrix, K_{uu} is the structural stiffness matrix, $K_{u\phi}$ is the piezoelectric coupling matrix, $K_{\phi\phi}$ is the dielectric stiffness matrix, and a superscript T denotes transpose of a matrix; F_u denotes the structural load and F_ϕ denotes the electric load.

In practical application of structural analysis, damping matrix C_{uu} is usually assumed to be a linear combination of the structural mass matrix M_{uu} and the structural stiffness matrix K_{uu}:

$$C_{uu} = aM_{uu} + bK_{uu}. \tag{4}$$

The knowledge of natural frequencies and corresponding mode shapes is preferred for active vibration control design. A set of r vibration modes ($r \leqslant n$) can be solved by running a modal analysis based on Eq. (3) with damping neglected. Each mode corresponds to a natural frequency ω_i and a mode shape vector Φ_i ($i = 1, 2, \ldots, r$). The size of r is selected depending on the type of structure considered [12].

Let X denote modal generalized displacements. A change of basis is carried out using

$$\begin{pmatrix} u \\ \phi \end{pmatrix} = [\Phi](X). \tag{5}$$

The dynamic equilibrium equation (3) can now be converted to modal-space model as

$$(\ddot{X}) + \left[\Phi^{\mathrm{T}}\right] \begin{bmatrix} C_{uu} & 0 \\ 0 & 0 \end{bmatrix} [\Phi][\dot{X}] + \Omega^2(X) = \left[\Phi^{\mathrm{T}}\right] \begin{pmatrix} F_u \\ F_\phi \end{pmatrix}, \tag{6}$$

where $\Omega^2 = \mathrm{diag}[\omega_1^2 \omega_2^2 \cdots \omega_r^2]$, and the modal matrix $[\Phi]$ has been normalized with respect to mass.

Note that the dynamic equilibrium equation (6) decouples into r equations corresponding to each individual mode, provided the damping is proportional as described by Eq. (4).

3. Optimal control design

The design of active control system is carried out in state space form. The second-order equation (6) can be converted to a standard first-order state space model as

$$\dot{x} = Ax + Bu_{\mathrm{c}}, \tag{7}$$

which represents

$$\begin{pmatrix} \dot{X}_1 \\ \ddot{X}_1 \\ \dot{X}_2 \\ \ddot{X}_2 \\ \cdots \\ \cdots \end{pmatrix} = \begin{pmatrix} 0 & 1 & 0 & 0 & \cdots & \cdots \\ -\omega_1^2 & -2\xi_1\omega_1 & 0 & 0 & \cdots & \cdots \\ 0 & 0 & 0 & 1 & \cdots & \cdots \\ 0 & 0 & -\omega_2^2 & -2\xi_2\omega_2 & \cdots & \cdots \\ \cdots & \cdots & \cdots & \cdots & \cdots & \cdots \\ \cdots & \cdots & \cdots & \cdots & \cdots & \cdots \end{pmatrix} \begin{pmatrix} X_1 \\ \dot{X}_1 \\ X_2 \\ \dot{X}_2 \\ \cdots \\ \cdots \end{pmatrix} + \left[\Phi^{\mathrm{T}}\right] \begin{pmatrix} 0 \\ F_\phi^{\mathrm{c}} \end{pmatrix}, \tag{8}$$

where X_i denotes the generalized displacement of i-mode as indicated in Eq. (5), ξ_i is conventionally defined damping ratio for the ith mode, F_ϕ^{c} denotes applied control force in terms of electric load.

Note that application loads have been omitted in system equations (7) and (8). Control force F_ϕ^{c} in Eq. (8) is taken as a pure feedback with no auxiliary input. It may be necessary to add noise terms to represent process and measurement noises in practical applications. It is also noted that a model size reduction technique is necessary in design practice of complex real-life structures to determine the smallest state space model while keeping accurate representation of the frequency response characteristics [13].

Sensor-measured output can be expressed in state space form as

$$y = Cx, \tag{9}$$

where output matrix C is the function of modal matrix $[\Phi]$ and sensor locations.

Both coupled control and independent control methods can be employed for active structural control [14]. The independent modal-space control (IMSC) method is one-loop-at-a-time procedure of classical control design. It is efficient only when the control of a few modes is of interest.

Coupled control is desirable when simultaneous control of multimodes is required. Two feedback control laws are available for coupled control design: state feedback and output feedback. Linear quadratic regulator (LQR) is usually employed to determine the feedback gain. The feedback gain K is chosen to minimize a quadratic cost or performance index (PI) of the form

$$J = \frac{1}{2}\int_0^\infty (x^{\mathrm{T}} Q x + u_{\mathrm{c}}^{\mathrm{T}} R u_{\mathrm{c}})\,\mathrm{d}t, \tag{10}$$

where Q and R are symmetric positive semidefinite weighting matrices, and their elements are selected to provide suitable performance.

State feedback requires a full knowledge of states

$$u_{\mathrm{c}} = -Kx. \tag{11}$$

The determination of control gain K in Eq. (11) can be reduced to solving a matrix Riccati equation [15]

$$A^{\mathrm{T}}P + PA - PBR^{-1}B^{\mathrm{T}}P + Q = 0, \tag{12}$$

where matrices A and B are defined in Eq. (7), P is an auxiliary matrix.

The control gain for state feedback is then obtained by

$$K = R^{-1}B^{\mathrm{T}}P. \tag{13}$$

Not all the state components are always available for feedback purpose in practical design problems. A full knowledge of states has to be estimated based on sensor measurements in order to implement state feedback control. Alternatively, output feedback control provides a more meaningful design approach in practice. Measured output (y) from sensors are directly fed back to actuators through

$$u_{\mathrm{c}} = -Ky. \tag{14}$$

Design equations for output feedback control are more complicated compared to state feedback control. Substitution of Eqs. (9) and (14) into (7) results in the controlled system equation

$$\dot{x} = (A - BKC)x = A_{\mathrm{c}}x. \tag{15}$$

The PI can be rewritten using Eqs. (9) and (14) as

$$J = \frac{1}{2}\int_0^\infty \left[x^{\mathrm{T}}\left(Qx + C^{\mathrm{T}}K^{\mathrm{T}}RKC\right)x\right]\,\mathrm{d}t. \tag{16}$$

The problem of output feedback control design is now to select the control gain K so that the cost J given by Eq. (16) is minimized, subjected to the dynamical constraint of Eq. (15). By introducing two auxiliary matrices P and S, the dynamical optimization problem can be reduced to solving three coupled equations [15]:

$$A_{\mathrm{c}}^{\mathrm{T}}P + PA_{\mathrm{c}} + C^{\mathrm{T}}K^{\mathrm{T}}RKC + Q = 0, \tag{17}$$

$$A_{\mathrm{c}}S + SA_{\mathrm{c}}^{\mathrm{T}} + X(0) = 0, \tag{18}$$

$$K = R^{-1}B^{\mathrm{T}}PSC^{\mathrm{T}}(CSC^{\mathrm{T}})^{-1}, \tag{19}$$

where $X(0)$ is a function of initial state: $X(0) = x(0)x^{\mathrm{T}}(0)$.

Eqs. (17) and (18) are Lyapunov equations. The dependence of optimal gain on the initial state is undesirable but typical of output feedback control design [15]. Uniformly distributed initial states can be assumed in practice. The iterative solution algorithm presented by Moerder and Calise [16] can be used to solve the three equations (17)–(19) and determine the optimal output feedback control gain K.

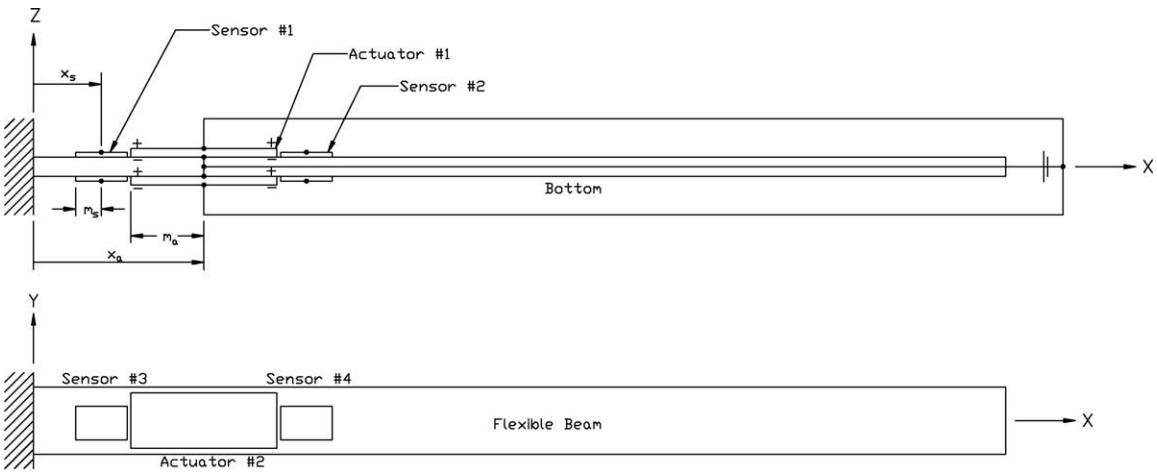

(a)

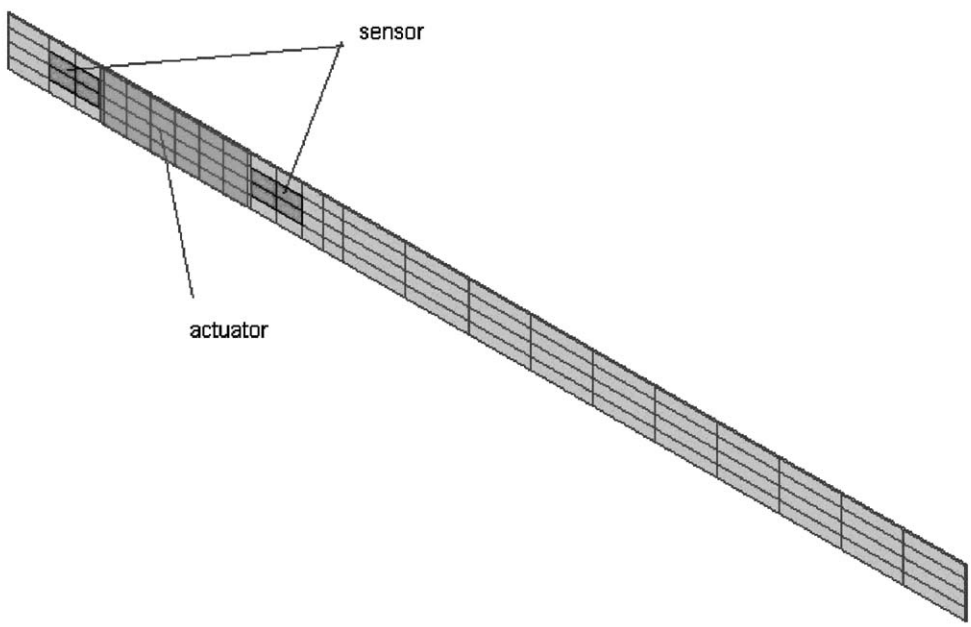

(b)

Fig. 1. Configuration of experimental beam. (a) Physical model and (b) finite element model.

Table 1
Natural frequencies of the experimental beam

Mode	Natural frequencies (Hz)		
	Experimental [17]	SMARTCOM [18]	Present study
I	3.41	3.08	3.11
II	16.90	15.89	16.07

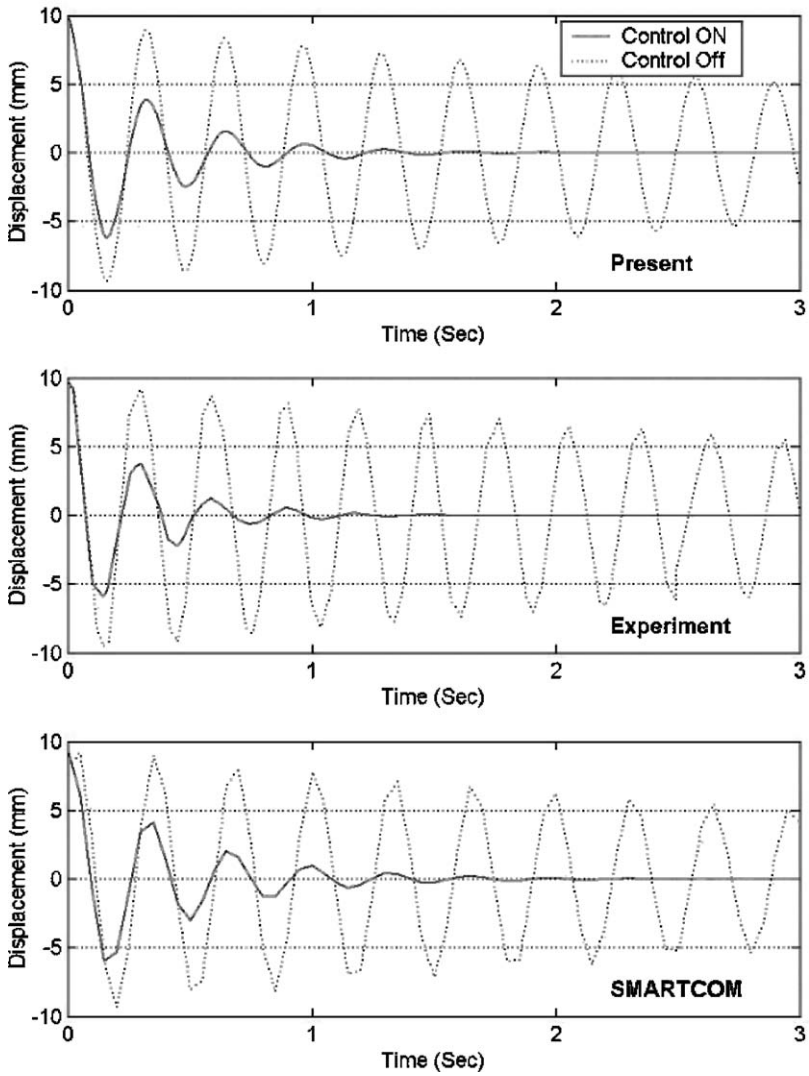

Fig. 2. Tip displacement response of the experimental beam.

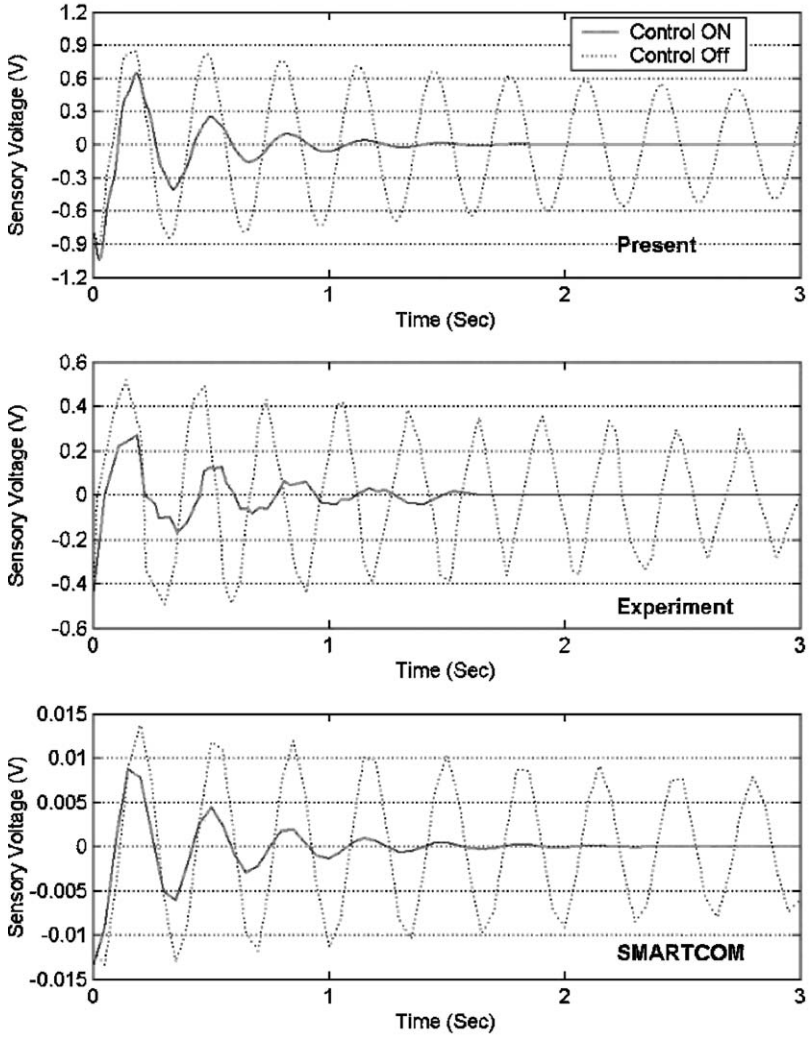

Fig. 3. Sensory voltage at the center of sensor #1 of the experimental beam.

The selection of weighting matrices Q and R is vital in the control design process. The relative magnitudes of Q and R are selected to trade off requirements on the smallness of the state against requirements on the smallness of the control force. A larger Q puts higher demand on control result, and a larger R puts more limit on applied control force. An efficient way of choosing Q is to consider the objectives of control performance. For a proposed structure, a performance output z can be constructed in the form of [15]

$$z = Hx, \tag{20}$$

where performance output matrix H is the function of modal matrix and output location.

Performance output z is chosen based on desired control objective. For instance, for a cantilever beam with vertical load, tip vertical displacement can serve as performance output. Once z is set, the

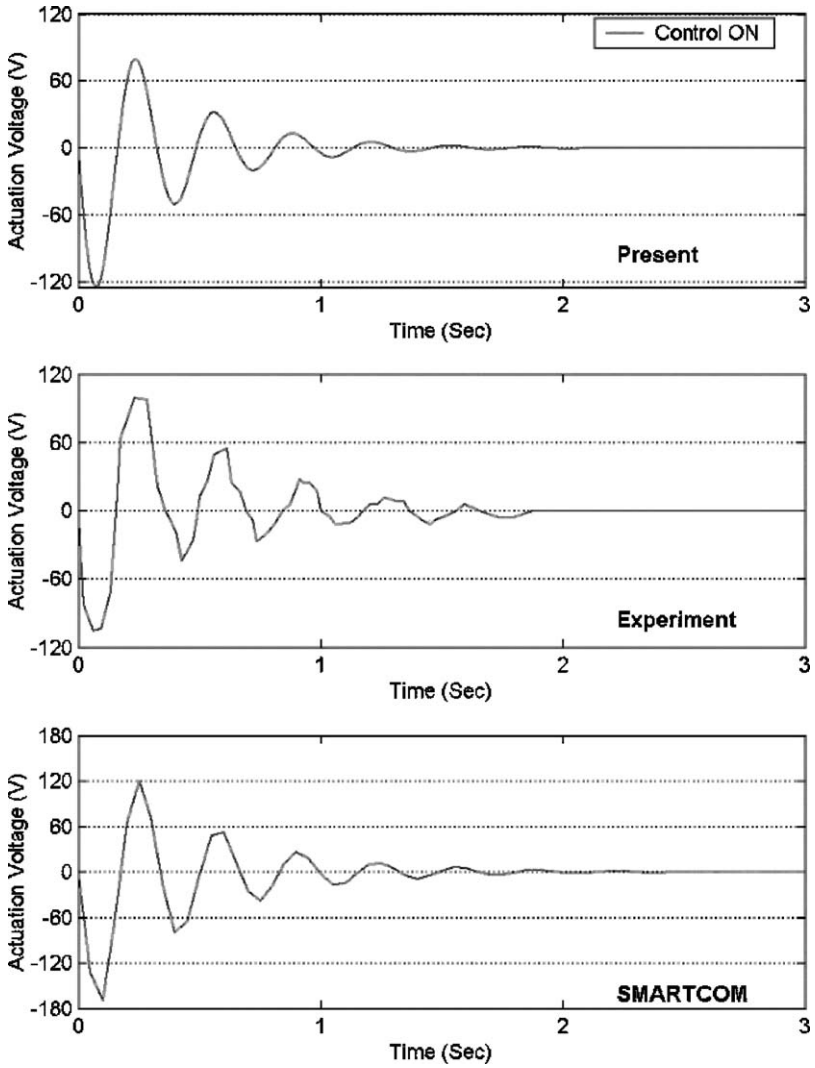

Fig. 4. Actuation voltage at the center of actuator #1of the experimental beam.

performance output matrix H can be determined. Weighting matrix Q can then be computed from H with $Q=H^{\mathrm{T}}H$. Weighting matrix R can be set as $\rho_{\mathrm{c}}I$ with ρ_{c} as a scalar design parameter. Therefore, the challenging task of choosing Q and R reduces to choosing one parameter ρ_{c}. Consequently, the control performance such as settling time can be tuned through changing the value of ρ_{c}. This procedure is used in the course of case studies presented next.

4. Case studies

Case studies are presented in this section to demonstrate the validity and efficiency of the above-proposed design scheme. Selected piezoelectric smart structure systems for active vibration control

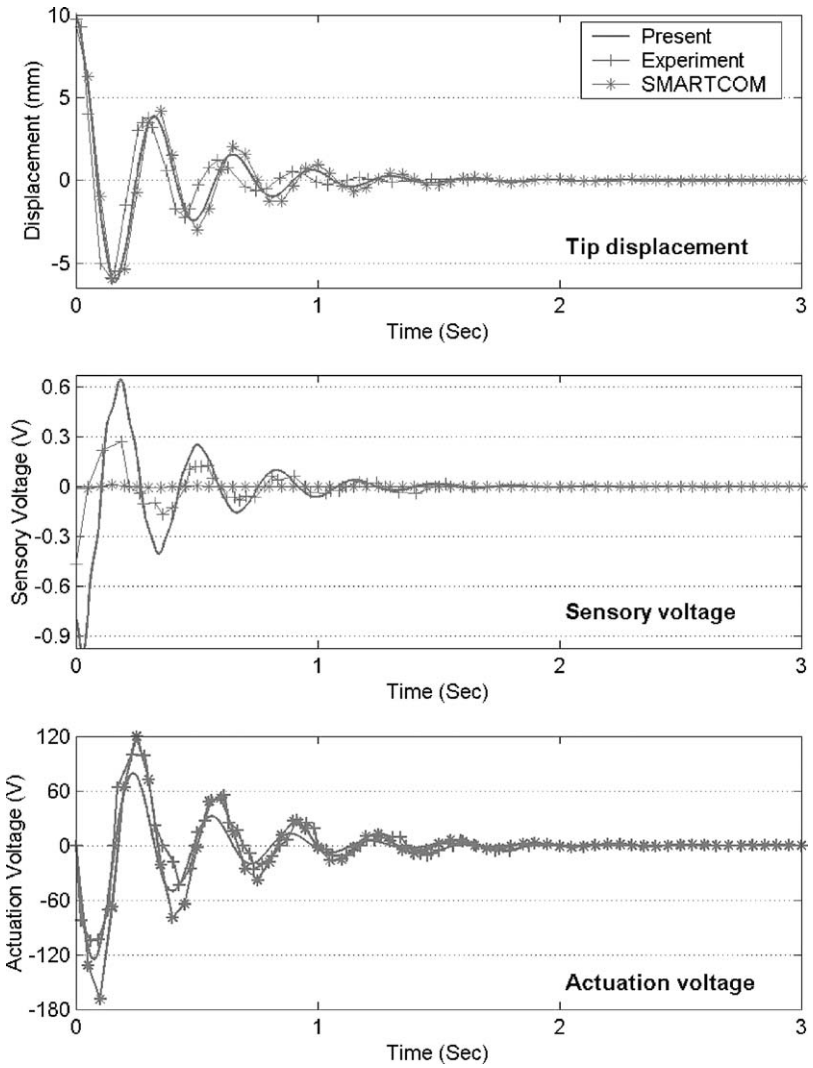

Fig. 5. Comparison of control performance of the experimental beam.

are designed using a commercial finite element code ANSYS (ANSYS 6.1) and output feedback control law. Three-dimensional coupled-field solid element (Solid 5) is utilized to model piezoelectric patches, and three-dimensional structural solid element (Solid 45) is employed to model host structures. Lyapunov equations (17) and (18) are solved by MATLAB Control System Toolbox (MATLAB 6).

4.1. An experimental beam structure

The flexible cantilevered beam structure (Fig. 1a) tested by Yousefi-Koma [17] is studied first. The structure consists of an aluminum beam ($508 \times 25.4 \times 0.8\ \text{mm}^3$) four PVDF piezofilm sensors

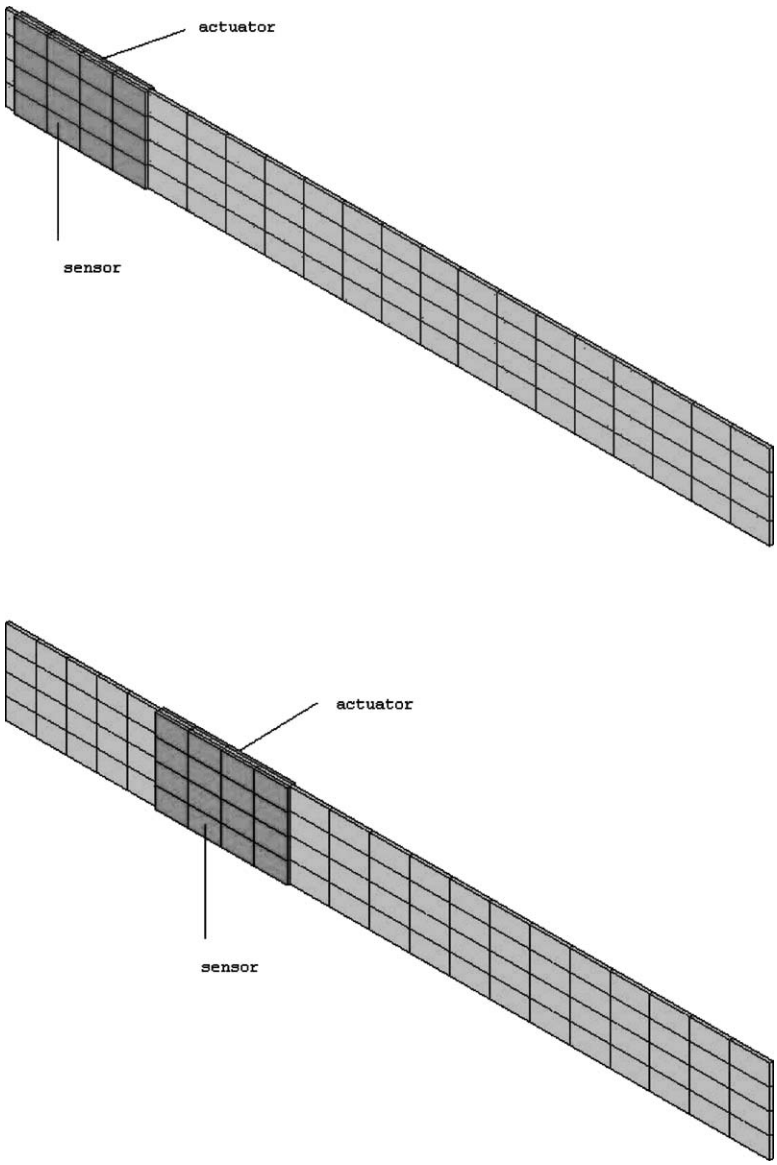

Fig. 6. Finite element model of cantilevered plate structure with piezoactuator/sensor: collocated configurations.

($27\times13\times0.028$ mm^3), and two PZT piezoceramic actuators ($76.2\times25.4\times0.305$ mm^3). Sensors #1, #2 and actuator #1 are bonded to the top surface of the host beam, while sensors #3, #4 and actuator #2 are symmetrically bonded to the bottom surface. All sensors and actuators are symmetrically located about the x-axis. Details of the configurations and material properties can be found at [17]. The finite element model of the beam structure is given in Fig. 1b.

The natural frequencies of the experimental beam structure for the first two modes are given in Table 1. The results from the in-house code SMARTCOM [18] and experimental results [17] are also

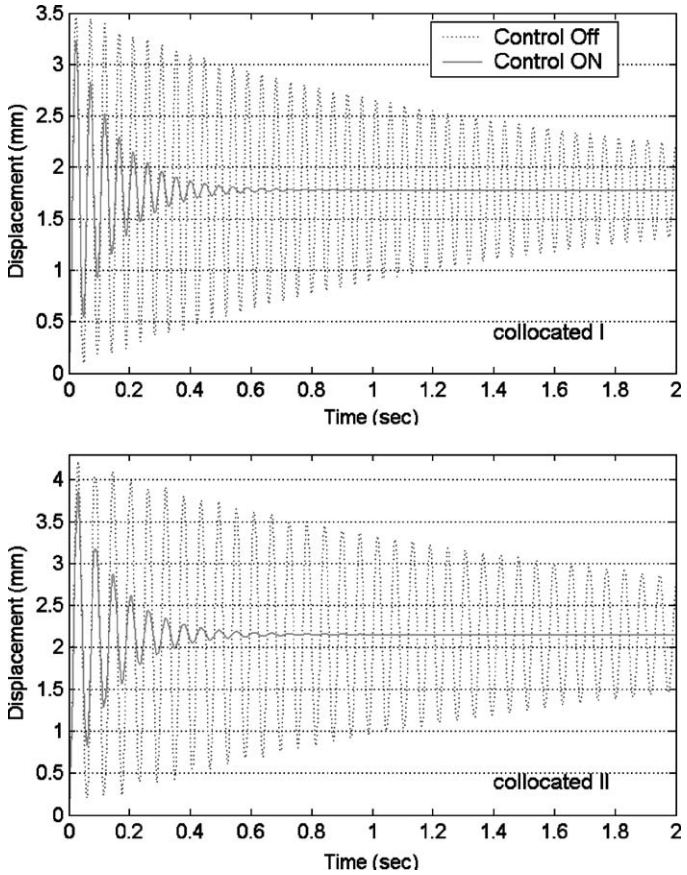

Fig. 7. Tip displacement response of cantilevered plate structure with piezoactuator/sensor: collocated configurations.

given for the purpose of comparison. It is seen that present results based on ANSYS are somewhat closer to the experimental data.

In the experimental study [17], the dynamic response of the beam structure was studied for a period of 3 s, under an initial tip displacement of 10 mm. The damping ratios for the first two modes were given as 0.011 and 0.055. The first 10 modes are included in the numerical simulation. Uniform damping ratio 5.5% is used except 1.1% for the first mode, based on the experimental data. The settling time of 1 s is used to design the controlled system. Tip vertical displacement is selected as the performance output to determine weighting matrix Q.

The dynamic response of the controlled beam structure are presented in Figs. 2–4. Corresponding results from the experimental study and SMARTCOM are also presented. Fig. 2 shows the vertical displacement at the beam tip for the case with and without active control. Fig. 3 plots sensory feedback voltage at the center of sensor #1, while Fig. 4 plots the applied actuation voltage at the center of actuator #1. The control results from present study, the experimental study and SMARTCOM are compared in Fig. 5. Fairly good agreements on structural tip displacement and applied control force are observed between three results.

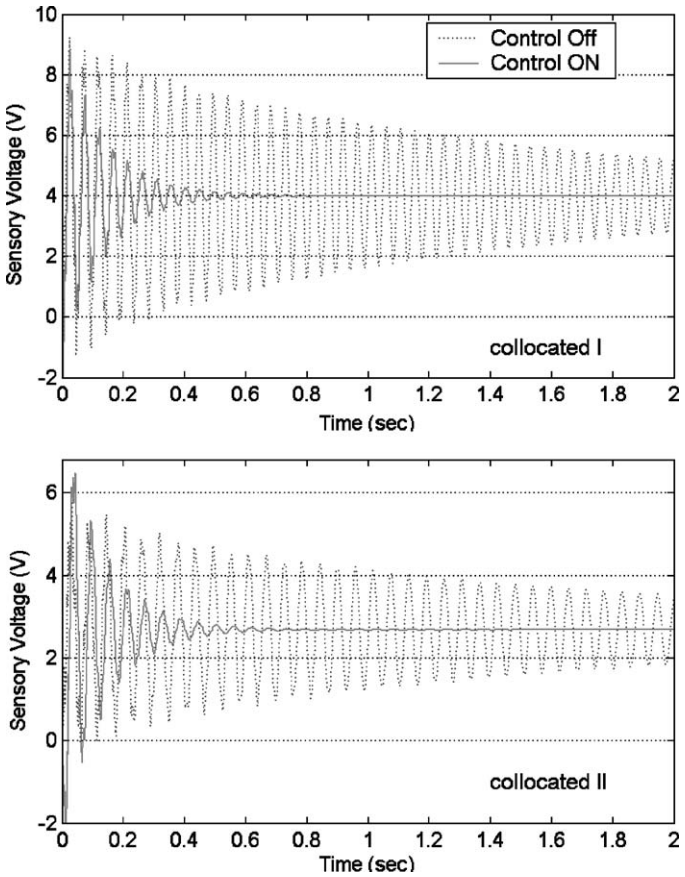

Fig. 8. Sensor response of cantilevered plate structure with piezoactuator/sensor: collocated configurations.

4.2. A cantilevered plate structure

A cantilevered plate structure is studied next. The structure consists of a host aluminum plate ($226 \times 25 \times 0.965$ mm^3), a PZT-5H sensor ($39 \times 25 \times 0.75$ mm^3), and a PZT-5H actuator ($39 \times 25 \times 0.75$ mm^3). The sensor and actuator are perfectly bonded to the upper or lower plate surfaces. To examine the effect of sensor and actuator locations on the control performance, the plate structure is studied for four different sensor/actuator configurations: collocated cases I and II, and non-collocated cases I and II. Note that the system of collocated case I was studied by Lim et al. [19], but the issue of designing feedback control was not examined in their study; Smith et al. [8] discussed the state feedback design of a system similar to non-collocated case II, where detailed information about locations of sensor/actuator was not given. The material properties of PZT-5H and aluminum are given below [19].

PZT-5H:

$c_{11} = 12.6 \times 10^{10}$ N/m^2, $c_{12} = 7.95 \times 10^{10}$ N/m^2, $c_{13} = 8.41 \times 10^{10}$ N/m^2,
$c_{33} = 11.7 \times 10^{10}$ N/m^2, $c_{44} = 2.33 \times 10^{10}$ N/m^2,

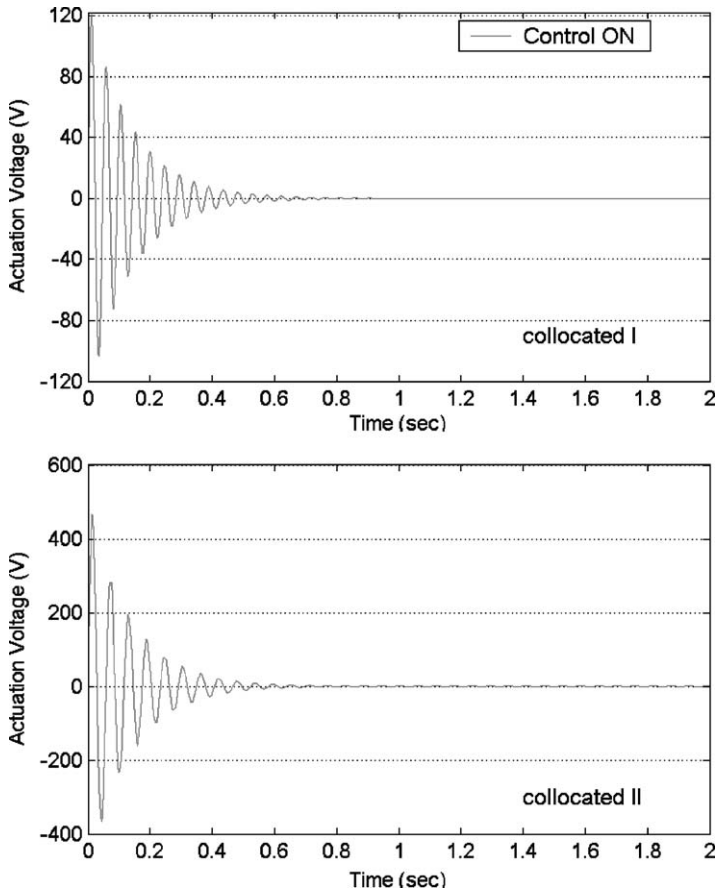

Fig. 9. Applied control force response of cantilevered plate structure with piezoactuator/sensor: collocated configurations.

$e_{31} = -6.5$ C/m^2, $e_{33} = 23.3$ C/m^2, $e_{15} = 17$ C/m^2,
$\epsilon_{11} = 1.503 \times 10^{-8}$ C V/m, $\epsilon_{33} = 1.503 \times 10^{-8}$ C V/m,
Density $\rho = 7500$ kg/m^3.

Aluminum:
Young's modulus $E = 68$ GPa, Poisson's ratio $v = 0.32$,
Density $\rho = 2800$ kg/m^3.

Fig. 6 shows the finite element models of two collocated configurations. The two configurations differ in the distance from sensor/actuator to the clamped end. The centers of piezoelectric patches in case I are 22.5 mm away from the clamped end, and they are 64.5 mm away from the clamped end in case II. The dynamic response of the plate structure is studied under a step load of 0.1 N applied at the free end. The first 10 modes are included in the numerical simulation. Uniform structural damping with a typical value of 0.5% is assumed. Vertical displacement at the plate tip is selected as the performance output. A settling time of 0.4 s is used to design the control.

Transient responses of the plate tip displacement are shown in Fig. 7. Results when the control is off are also shown for comparison. Corresponding sensory feedback voltages at the center of the

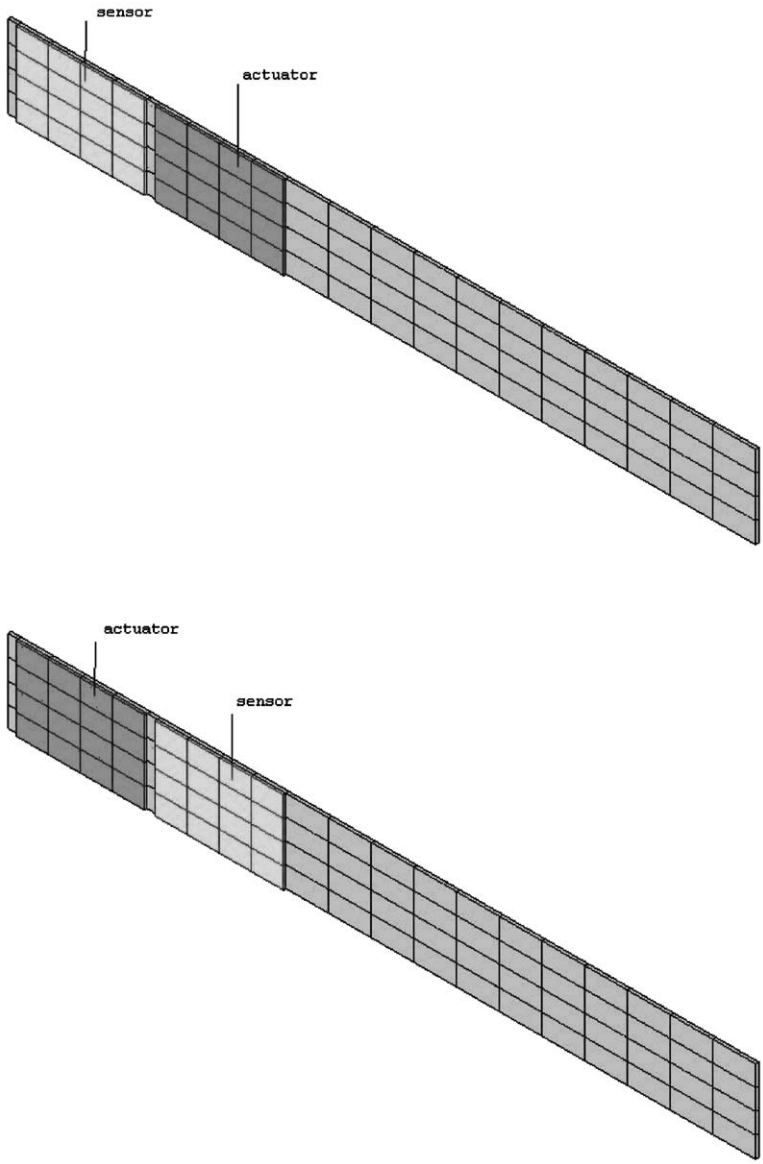

Fig. 10. Finite element model of cantilevered plate structure with piezoactuator/sensor: non-collocated configurations.

sensor are plotted in Fig. 8, and applied actuation voltages at the center of the actuator are plotted in Fig. 9. Collocated case I requires control force of 120 V to achieve the settling time of 0.4 s, while up to 450 V control force is required for collocated case II. The influence of sensor/actuator location on the integrated system and control design is clearly evident.

Two non-collocated configurations are considered in Fig. 10. The sensor and actuator locations in non-collocated case I are interchanged with those in non-collocated case II. Note that the actuator in case II is 42 mm closer to the clamped end. The systems are designed under the same conditions as

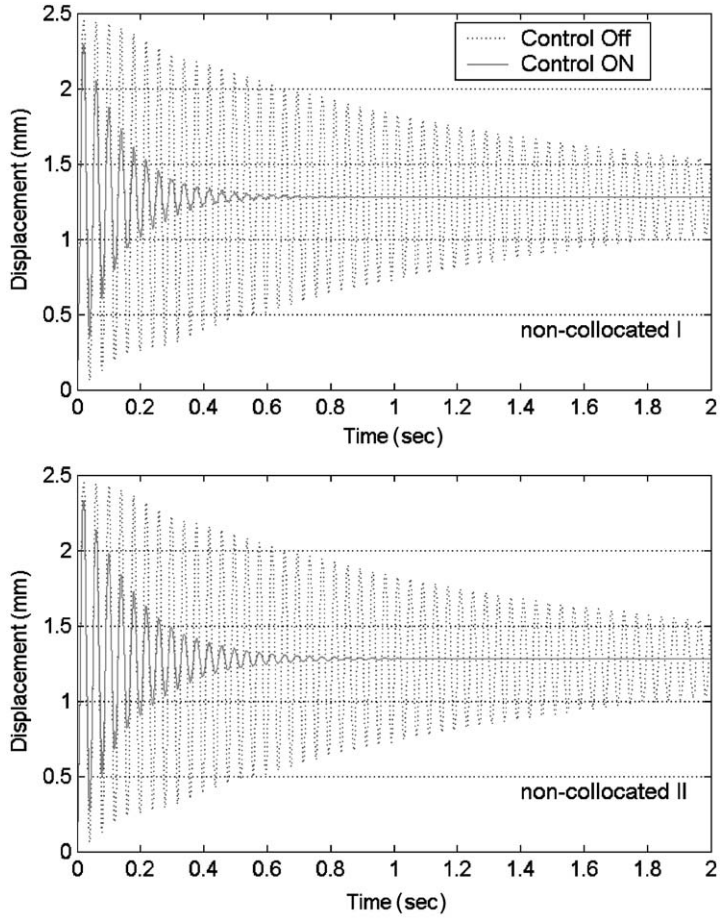

Fig. 11. Tip displacement response of cantilevered plate structure with piezoactuator/sensor: non-collocated configurations.

in collocated cases. The plate tip displacement, sensor response and actuation voltage are shown in Figs. 11, 12 and 13, respectively. As expected, the two systems have identical displacement response with or without active control. However, sensor response and required actuator force are different in two cases. Non-collocated case I requires almost double control force compared to non-collocated case II. The control is more efficient when the actuator is closer to the clamped end.

The performances of four configuration cases are compared in Table 2. Among all four cases, collocated case II requires the highest control force (450 V) to achieve the settling time of 0.4 s, and non-collocated case II requires the least control force (40 V). This can be explained with differences in structure natural settling time and actuator placement. Note that structure natural settling time corresponds to the state when active control is turned off, and the structure vibration is solely suppressed by structural damping (0.5% ratio in the present case). Natural settling time is therefore an intrinsic parameter of a structure. Collocated configuration case II has the highest value of natural settling time (5.4 s), and therefore demands more control force to achieve the targeted active settling time 0.4 s. Two non-collocated configuration cases I and II have identical natural settling time (3.7 s),

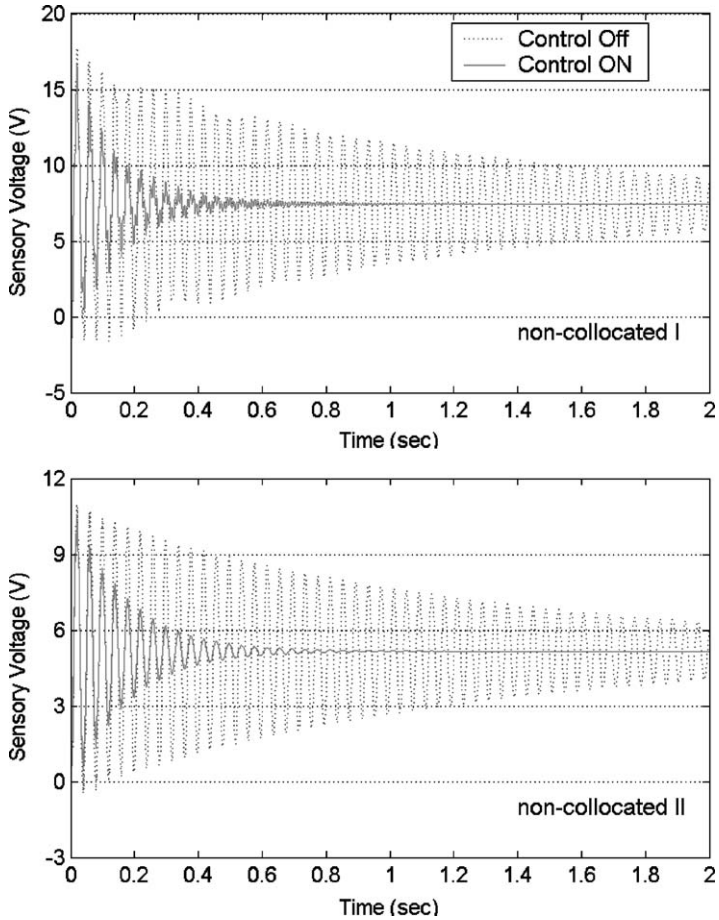

Fig. 12. Sensor response of cantilevered plate structure with piezoactuator/sensor: non-collocated configurations.

but require different control force to achieve targeted active settling time 0.4 s. The case with actuator closer to the clamped end (case II) requires less control force. Same conclusion can be drawn when comparing collocated case I with case II. Therefore, for clamped structures, the closer the actuator is to the clamped end, the more efficient is the control. The fact that different sensor/actuator placements result in different control performance suggests the importance of analyzing the integrated structure and performing parameter studies to identify optimal design with maximum control effect in practice design. In addition, it is interested to note that the maximum sensory voltage in collocated case II (Fig. 8) has a higher value when the control is on compared to when the control is off. This is the reflection of applied strong control force on the actuator.

A further study is conducted on non-collocated configuration case II. The correlation between required control force and the settling time is studied by designing the control system under 10 different settling time, i.e. 0.1, 0.2, ..., 1.0 (s). The results are plotted in Fig. 14. Similar results are presented by Smith et al. [8] using SMARTCOM. It is reasonable to see that control force decreases with increasing value of settling time. Note that decreasing rate is higher when the value of settling

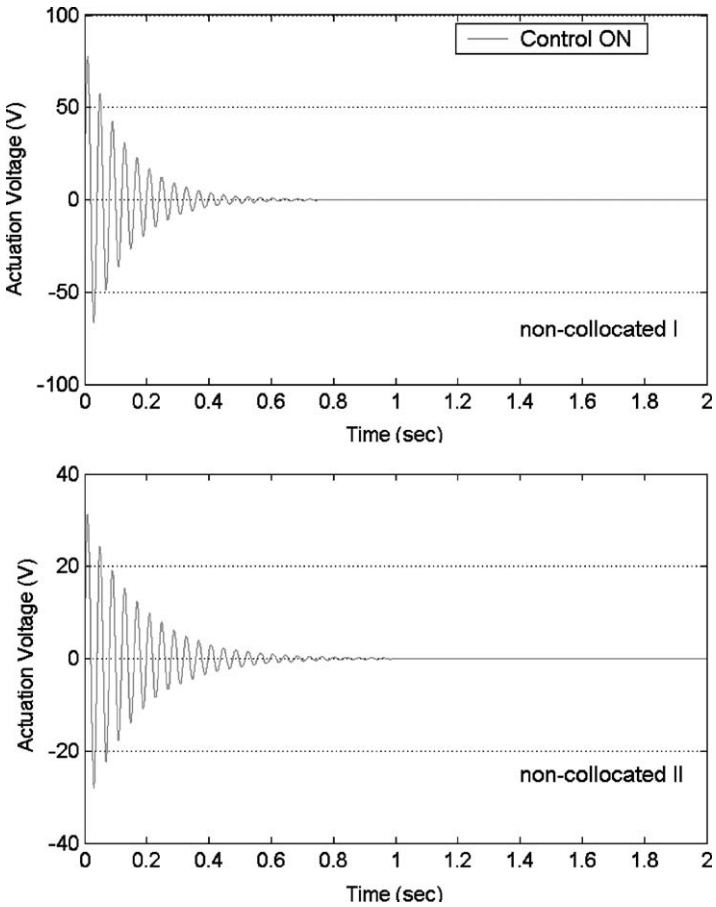

Fig. 13. Applied control force response of cantilevered plate structure with piezoactuator/sensor: non-collocated configurations.

Table 2
Performance comparisons of four cantilevered plate structures with different piezoelectric sensor/actuator locations (design under identical settling time $T_s = 0.4$ s)

Case		Collocated I	Collocated II	Non-collocated I	Non-collocated II
Natural settling time (s)		4.4	5.4	3.7	3.7
Maximum actuation voltage (V)		120	450	75	40
Maximum sensory voltage (V)	Control off	9	5.8	17	11
	Control on	8.5	6.2	16	10
Maximum tip displacement (mm)	Control off	3.5	4.2	2.4	2.4
	Control on	3.2	3.8	2.3	2.3

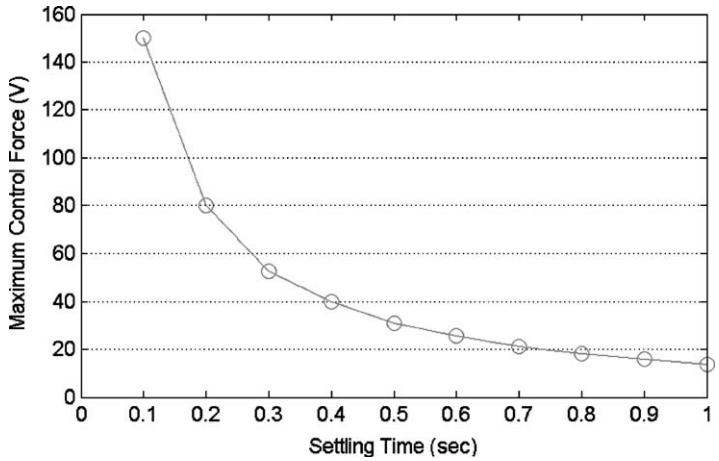

Fig. 14. Maximum actuation voltages as a function of settling time for the cantilevered plate with piezoactuator/sensor (non-collocated configuration—case II).

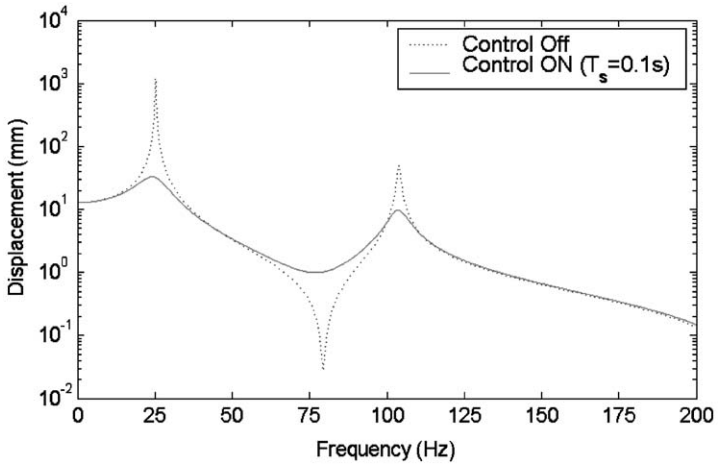

Fig. 15. Frequency spectrum at the tip of cantilevered plate with piezoactuator/sensor (non-collocated configuration—case II).

time is small. Such curve can be useful to seek a balance between the control effort and the control result in practical design of actively controlled structures.

Fig. 15 presents the frequency response (bode plot) at the plate tip under applied point force for the non-collocated case II. The control results of the first two modes with a settling time $T_s = 0.1$ s are within the plotted frequency range (0–200 Hz). The comparison of controlled response with uncontrolled response clearly indicates that the amplitude is greatly reduced by the active control force.

In practical design practice, it is important to ensure that the maximum voltages on sensors and actuators are within certain ranges so that piezoelectric patches will not experience electric breakdown. Note that these ranges are predefined based on material properties and device characteristics.

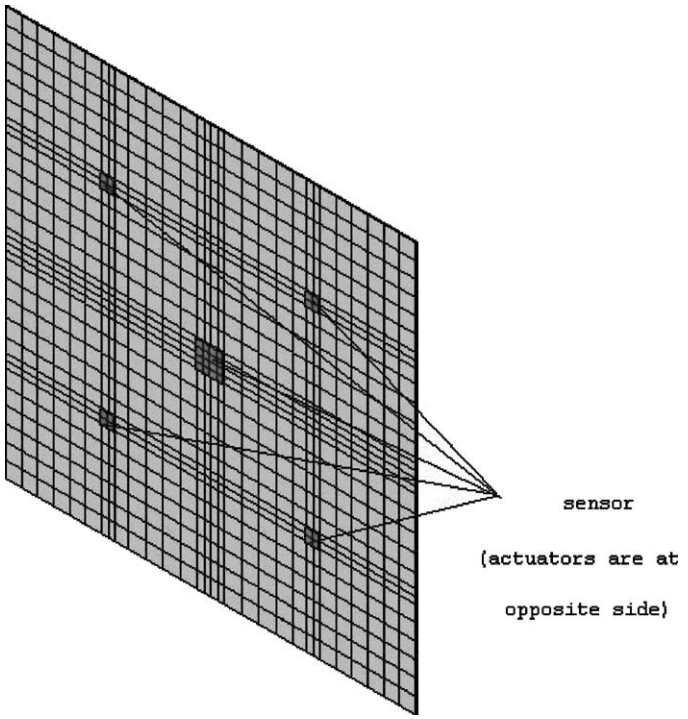

Fig. 16. Finite element model of a clamped plate with piezoactuator/sensor.

If the linear piezoelectric constitutive equations are used to design the structures as in present study, it is also imperative to restrict sensor and actuator voltages within the linear range. The maximum actuation voltage in collocated configuration case II is 450 V, which probably exceeds the linear range of most piezoelectric ceramics. To maintain linear piezoelectric behavior, the targeted active settling time 0.4 s should be relaxed or an additional actuator is needed. Such considerations are not implemented here for brevity.

4.3. A clamped plate structure

Finally, a clamped plate structure is studied. The host structure is an aluminum plate ($305 \times 303 \times 0.8\ \text{mm}^3$). Five patches of PZT-5H sensors are bonded to the upper surfaces of the plate. One sensor ($20 \times 20 \times 1\ \text{mm}^3$) is located at the center of the plate, and four sensors of equal size ($10 \times 10 \times 1\ \text{mm}^3$) are located along the diagonal of the plate. Five patches of PZT-5H actuators are collocately bonded on the lower surface of the plate. Fig. 16 shows the finite element model of the structure. A similar structure was studied by Lim et al. [9] using an inhouse code. As noted by Lim et al. [9], sensors and actuators are placed at regions where strains are high to achieve high efficiency of actuation.

Consider an impulse load of 0.1 N applied at point (76.25 mm, 213.75 mm, 0.8 mm). Assuming structural damping is uniform and of value 0.01%, the dynamic response of vertical displacement at the center of the plate is plotted in Fig. 17a. The structure system is designed to suppress the

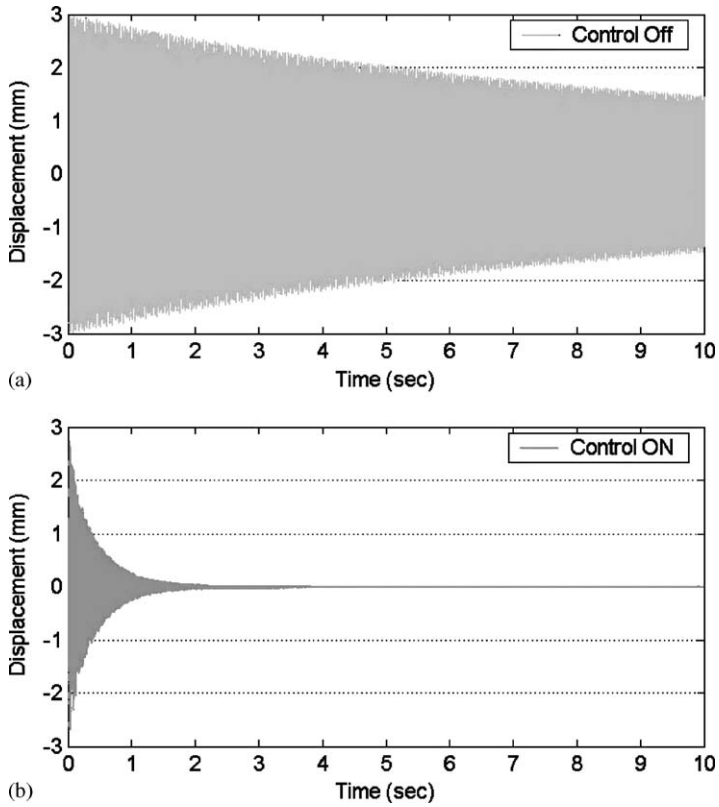

Fig. 17. (a,b) Vertical displacement response at the center of the clamped plate structure.

vertical vibration due to the impulse load. Choose vertical displacement at the plate center as the performance output, and set design parameter $\rho_c = 1.0 \times 10^{-10}$. The controlled displacement response is shown in Fig. 17b. The active settling time is found to be 1.34 s, which is 43 times less than the structure natural settling time 57.9 s. Note that piezoelectric patches only add 5.8% mass to the plate structure. This example, therefore, demonstrates that high efficient vibration control can be achieved using bonded piezoelectric patches with only a small impact on structure weight.

5. Conclusions

A general purpose scheme of analyzing/designing actively controlled smart structures with piezoelectric sensors and actuators is successfully developed in this study. The present scheme has the flexibility of using any piezoelectric finite element code and a user-selected feedback control law. The validity and efficiency of present scheme is confirmed by comparing with available results reported in the literature.

Numerical results indicate that the locations of piezoelectric sensors and actuators may have significant influence on the integrated system and control performance. Proper placement of sensors and

actuators should be sought in practical design practice through parameter studies to identify optimal control design for maximum control effect. It is feasible to design an efficient controlled structure system with piezoelectric patches having minor impact on structure weight.

Acknowledgements

The work of SXX was supported by the Canadian National Science and Engineering Research Council (NSERC) through an Industrial Research Fellowship (IRF) program. The support of Martec Limited is also acknowledged. SXX is grateful to Dr. Eric Anderson and Dr. Roger Glaese from CSA Engineering for their helpful discussions on feedback control design. Special thanks to Mr. Keith Gallant for his assistance in collecting data from [17] and [18] used in Figs. 2–5.

References

[1] C.A. Rogers, Intelligent material systems—the dawn of a new materials age, Sci. Mach. J. 46 (1994) 977–983.
[2] M. Sunar, S.S. Rao, Recent advances in sensing and control of flexible structures via piezoelectric materials technology, Appl. Mech. Rev. 52 (1999) 1–16.
[3] A.V. Srinivasan, D.M. McFarland, Smart Structures: Analysis and Design, University Press, Cambridge, 2001.
[4] A. Benjeddou, Advances in piezoelectric finite element modeling of adaptive structural elements: a survey, Comput. Struct. 76 (2000) 347–363.
[5] H.S. Tzou, C.I. Tseng, Distributed piezoelectric sensor/actuator design for dynamic measurement/control of distributed parameter systems: a piezoelectric finite element approach, J. Sound Vib. 138 (1990) 17–34.
[6] S.K. Ha, C. Keilers, F.K. Chang, Finite element analysis of composite structures containing distributed piezoelectric sensors and actuators, AIAA J. 30 (1992) 772–780.
[7] T.S. Koko, I.R. Orisamolu, M.J. Smith, U.O. Alepan, Finite element based design tool for smart composite structures, Proc. SPIE Conf. Smart Struct. Mater. 3039 (1997) 125–134.
[8] M.J. Smith, T.S. Koko, I.R. Orisamolu, Comparative assessment of optimal control methods with integrated performance constraints, ASME Int. Mech. Eng. Congr. Exposition Adaptive Struct. Mater. Systems AD-Vol.57/MD-Vol.83 (1998) 141–148.
[9] Y.-H. Lim, S.V. Gopinathan, V.V. Varadan, V.K. Varadan, Vibration and noise control using an optimal output feedback controller, Proc. SPIE Conf. Smart Struct. Mater. 3667 (1999) 34–44.
[10] M.V. Gandhi, B.S. Thompson, Smart Materials and Structures, Chapman & Hall, London, 1992.
[11] J.M. Crowley, Fundamentals of Applied Electrostatics, Wiley, New York, 1986.
[12] K.J. Bathe, Finite Element Procedure, Prentice-Hall, Englewood Cliffs, NJ, 1996.
[13] M.R. Hatch, Vibration Simulation using MATLAB and ANSYS, CRC Press, LLC, Boca Raton, FL, 2000.
[14] L. Meirovitch, Dynamics and Control of Structures, Wiley, New York, 1990.
[15] F. Lewis, V.L. Syrmos, Optimal Control, Wiley, New York, 1995.
[16] D.D. Moerder, A.J. Calise, Convergence of a numerical algorithm for calculating optimal output feedback gains, IEEE Trans. Autom. Control AC-30 (1985) 900–903.
[17] A. Yousefi-Koma, Active vibration control of smart structures using piezoelements, Ph.D. Thesis, Carleton University, 1997.
[18] T.S. Koko, M.J. Smith, I.R. Orisamolu, Fuzzy and probabilistic design tool for actively controller smart composite structures: finite element and control capabilities, Martec Report TR-98-32, 1998.
[19] Y.-H. Lim, V.V. Varadan, V.K. Varadan, Closed loop finite-element modeling of active/passive damping in structural vibration control, Proc. SPIE Conf. Smart Struct. Mater. 3039 (1997) 113–124.